Surfaces and Interfaces 64 (2025) 106415

Contents lists available at ScienceDirect

Surfaces and Interfaces

journal homepage: www.sciencedirect.com/journal/surfaces-and-interfaces

Atomic layer deposition of hafnium dioxide for increasing temporal stability of silver-capped silicon nanopillar substrates used for SERS

Giulia Zappalà [a,*], Lasse Højlund Eklund Thamdrup [a], AmirAli Abbaspourmani [b], Elodie Dumont [a], Kaiyu Wu [c], Evgeniy Shkondin [d], Reyes Mallada [e], Maria Pilar Pina [e], Tomas Rindzevicius [a,b], Anja Boisen [a,*]

[a] The Danish National Research Foundation and Villum Foundation's Center for Intelligent Drug Delivery and Sensing Using Microcontainers and Nanomechanics (IDUN), Department of Health Technology, Technical University of Denmark, Denmark
[b] Silmeco ApS, 2450 Copenhagen, Denmark
[c] Shanghai Jiao Tong University, Shanghai, Minhang District, China
[d] National Centre for Nano Fabrication and Characterization, Technical University of Denmark, Denmark
[e] Instituto de Nanociencia y Materiales de Aragón (INMA), CSIC-Universidad de Zaragoza, 50009 Zaragoza, Spain

ARTICLE INFO

Keywords:
Surface-enhanced Raman spectroscopy
Atomic layer deposition
Thin protective coatings
Explosive detection
Plasmonic silver nanoparticles

ABSTRACT

Surface-enhanced Raman spectroscopy (SERS) is a label-free optical method employed due to its sensitivity and specificity. Metal nanoparticles are commonly used as SERS substrates for detection of molecules and any change in the metal affect the SERS performance. Silver (Ag) is a renowned plasmonic material, but it presents relatively poor chemical stability. The application of thin surface coatings has been recognized as an effective approach to enhance the chemical stability of Ag nanostructures, while preserving their desirable sensitivity.

Therefore, in this study 0–13 nm thick hafnium dioxide (HfO_2) coatings, deposited by atomic layer deposition (ALD), have been investigated to improve the temporal stability of Ag-capped silicon nanopillar (NP) SERS substrates. Comprehensive characterization was performed, and the SERS performance were evaluated with two reporter molecules on uncoated Ag-capped NP substrates. They displayed significant variation over time, while substrates with ~1.5 nm HfO_2 exhibited superior signal stability and noise reduction. Over a 5-month period, substrate stability was tested for detection of the nitroaromatic explosive 2,4-dinitrophenol. The limit of detection (LoD) and limit of quantification (LoQ) of uncoated Ag-capped NPs varied significantly, whereas HfO_2-coated substrates maintained a stable SERS performance with limited variation in the LoD and LoQ, thereby ensuring consistent results.

1. Introduction

Surface-enhanced Raman spectroscopy (SERS) has manifested itself as an important analytical technique across various research fields due to its exceptional sensitivity and specificity [1]. SERS is a surface-sensitive technique based on Raman scattering, in which inelastic scattering of photons provides detailed information about molecular vibrations of analyte molecules [2]. In SERS, the Raman signal is generally enhanced by a factor of 10^4 - 10^8 which is attributed to both electromagnetic (EM) and chemical enhancement [3]. However, EM enhancement factors up to 10^{11} have been estimated for dimers of Ag NPs [4]. The EM enhancement is predominant and arises from the interaction between incident light and a nanostructured metal surface, in which the excitation of localized surface plasmons on the metal surface causes a redistribution and an increase in the local electromagnetic field strength [5]. The localized electromagnetic field is responsible for the enhanced Raman scattering signal of molecules residing on or very near the surface. The close proximity greatly amplifies the Raman signal of the analyte, allowing for more accurate detection and analysis [6]. SERS represents a robust analytical method that provides detailed information about the chemical fingerprint of a target analyte absorbed on nanostructured noble metal surfaces [6].

SERS substrates most commonly comprise the noble metals gold (Au) and silver (Ag) in the form of thin films, thick films with nanoscale porosity or roughness or ultimately nanoparticles having different morphologies [7]. Ag is an outstanding plasmonic material, particularly

* Corresponding authors.
E-mail addresses: giuzap@dtu.dk (G. Zappalà), aboi@dtu.dk (A. Boisen).

https://doi.org/10.1016/j.surfin.2025.106415
Received 27 February 2025; Received in revised form 28 March 2025; Accepted 5 April 2025
Available online 6 April 2025

effective in the visible and near-infrared regions of the electromagnetic spectrum [8]. This effectiveness is due to its minimal plasmonic damping, a loss of energy in the plasmonic system, which is significantly lower than that of metals such as Au and copper (Cu) [9]. Owing to this low plasmonic damping, Ag nanostructures exhibit excellent localised surface plasmon resonance (LSPR) properties, and a superior EM field enhancement factor [10]. However, the use of Ag as a plasmonic material for SERS is limited by its poor chemical stability and its irreversible morphological changes. In ambient air, Ag reacts with sulphur and oxygen species, leading to the gradual formation of thick layers of silver sulphide or silver oxide [11]. In aqueous environments, Ag can be subject to chemical and structural changes induced by dissolved oxygen, pH variations, and halide ions. Furthermore, Ag nanostructures are susceptible to degradation and decreased performance when exposed to light and heat [10]. All the aforementioned issues attenuate or impair the plasmonic properties of Ag and as a result Au is often favoured for SERS applications [12]. The deposition of very thin (i.e. sub-5 nm) surface coatings has been identified as an effective strategy to improve the structural and chemical stability of Ag nanostructures while maintaining acceptable sensitivity [13]. Au represents an ideal shell material for protecting Ag substrates from oxidation and contamination over time [14]. However, depositing a uniform Au layer on Ag in an aqueous Au^{3+} solution is challenging due to an instantaneous galvanic reaction that can corrode the Ag nanostructure. In order to achieve a uniform and stable coating a precise control of the deposition process is required [14,15]. One of the most widely used surface modification techniques with an excellent control over the coating thickness is atomic layer deposition (ALD) [13]. Thermal and plasma-enhanced ALD allows for low temperature (i.e. temperatures below 300 °C) deposition of conformal coatings [13,16]. During fabrication of SERS-active substrates, ALD has previously been employed for deposition of ultra-thin coatings comprising functional dielectric materials, which protect Ag nanostructures from aggregation, and surface contamination [16]. While deposition of thin protective coatings serve to protect the Ag, it will also lead to a reduction in the SERS sensitivity due to the increased gap between the metal surface and the analyte, which weakens the localized EM field enhancement and diminishes the intensity of the Raman signal [13]. Various oxides such as SiO_2 [17], TiO_2 [18], Al_2O_3 [19] and HfO_2 [20], have been employed as protective layers on SERS substrates comprising Ag nanoparticles [14–17]. Among these oxides, HfO_2 offers several advantages for SERS analysis including (i) chemical stability, which makes the substrate insoluble even in acidic solutions, and (ii) high melting point and low thermal conductivity, which allows for protecting the substrate from thermal damage caused by high-power lasers [20]. In addition, the use of protective HfO_2 layers would make it possible to address the study of substrate "reusability" after regeneration by heating. Due to the high melting point of HfO_2, the coated substrates can exhibit enhanced thermal stability and can be heated to release adsorbed molecules, effectively refreshing them for subsequent measurements [21,22]. This property, connected with real-time measurements and long-term detection platforms, is of utmost importance from practical applications [22]. Temporal stability is also essential for ensuring reliable and reproducible SERS measurements. It ensures that the SERS signal remains consistent over time, thereby enabling precise quantification of analyte concentrations [23]. Utilizing SERS for e.g. biosensing [24] or environmental monitoring [25] requires temporally stable measurements for real-scenario applications. An example can be the identification of explosives at very low concentrations in different environments [26]. The chemicals and toxic compounds from unexploded munitions can have a significant negative environmental impact since such residues can leak into water sources and soil thereby becoming an environmental hazard [27].

Therefore, in the present study, the impact on SERS performance associated with deposition of ultra-thin HfO_2 ALD coatings on Ag-capped Silicon (Si) nanopillar (NP) SERS substrates was evaluated based on label-free detection of a nitroaromatic explosive 2,4-dinitrophenol (DNP). We employed ALD to prepare samples with different HfO_2 thicknesses ranging from 0 to 13 nm. While ALD coatings have been explored in various plasmonic applications, their use on the NP-based SERS substrates fabricated following *Schmidt* et al. [28] has never been explored. Therefore, a comprehensive characterization of the substrates was performed using scanning electron microscopy (SEM), x-ray reflectometry analysis (XRR), x-ray photoelectron spectroscopy (XPS), and scanning transmission electron microscopy (STEM) coupled with x-ray energy-dispersive spectroscopy (EDS). Moreover, a 3D finite element method was employed to simulate the maximum electrical field enhancement associated with a dimer comprising Ag-capped Si NPs having HfO_2 thicknesses ranging from 1–6 nm. We experimentally investigated the SERS performance over a 12-weeks period in terms of (i) long-term signal stability, (ii) background noise reduction, and (iii) overall signal intensity using two reporter molecules, trans-1,2-bis (4-pyridyl)ethylene (BPE), and 4-Nitrothiophenol (4-NBT), which showed that substrates coated with ~1.5 nm HfO_2 performed best. In order to test the substrate stability in a realistic scenario, the detection of different DNP concentrations was investigated. This was done by comparing substrates with and without the HfO_2 coating at two discrete time points: i) immediately after substrate fabrication and ii) five months after the fabrication. Although HfO_2-coated substrates showed a reduced overall sensitivity, the test demonstrated a significant decrease in the SERS sensitivity of non-coated SERS substrates after a duration of five months. In contrast, HfO_2-coated substrates showed incredibly stable SERS performances, confirming that protective layers provide a feasible strategy to improve the structural and chemical stability of Ag-based SERS substrates.

2. Materials and methods

2.1. Fabrication process

In this study, Ag-capped Si NP SERS substrates covered with thin layers of HfO_2 were produced. As first outlined in *Schmidt* et al. [28], the substrate fabrication process comprises two steps: (i) maskless reactive ion etching (RIE) of Si and (ii) line-of-sight metal deposition using batch electron-beam deposition of Ag. In summary, single-side polished 6″ Si wafers (Siegert Wafer GmbH, Aachen, Germany) from stock were used. Prior to the RIE process, the platen temperature was reduced to 0 °C and allowed to stabilize before preconditioning the chamber by running the pre-optimized etching process on a clean dummy substrate. The etching was conducted on an inductively coupled plasma system (PRO ICP, SPTS a KLA company, Newport, United Kingdom) using a chamber pressure of 36 mTorr, $SF_6|O_2$ flow rates of 30|27 sccm, platen power of 120 W and a silicon etching time of 5 min 20 s. This resulted in Si NPs having a height and density of approximately 640 nm and 20 NPs/μm^2, respectively. In the second step, electron-beam deposition of 200 nm Ag (99.99 % purity, Testbourne B.V., Helmond, The Netherlands) was conducted on a batch deposition system (Temescal FC-2000, Ferrotec, Livermore, USA). During deposition, isolated plasmonic Ag caps are formed on the acute apices of the Si NPs. The e-beam deposition was executed with an initial chamber pressure below $1{\cdot}10^{-6}$ Torr and a deposition rate of 10 Å/s. To explore the impact of adding thin HfO_2 coatings on the produced SERS substrates, a third fabrication step was added: thermal ALD (Picosun R200, Picosun, Espoo, Finland) was employed to deposit HfO_2 coatings, exhibiting variable thicknesses, on the Ag-capped Si NP SERS substrates. The precursors used for the deposition were tetrakis(ethylmethylamido) hafnium (TEMAHf) and H_2O. The TEMAHf precursor was purchased from Strem Chemicals (Newburyport, Massachusetts, USA). It was initially heated to 125 °C for 120 min and the reactor temperature was set to 150 °C before starting the deposition process. During deposition the precursors (first TEMAHf, then H_2O) are introduced in the reaction chamber and the pulse|purge times was set to 1.6 s|60 s and 0.1 s|60 s for TEMAHf and H_2O, respectively. A specific boosted pulse program controls the 1.6 s pulse of the heated TEMAHf precursor: the pressure

inside the precursor container is initially increased by a carrier gas flow of 700 sccm for 1.2 s, then the flow is adjusted to 200 sccm, and the precursor is released in a 0.5 s pulse. The actual pulse duration is set 0.1 s shorter than the sum of these two phases. By increasing the number of deposition cycles, the HfO_2 thickness can be increased in a precise and reproducible manner. In total, 7 SERS substrates were subject to ALD deposition using 3, 6, 10, 15, 20, 25 and 150 cycles which resulted in HfO_2 thicknesses in the range from 0–13 nm. All the produced SERS substrates (with and without HfO_2 coating) were subsequently diced into 3 × 3 mm^2 chips using a laser micromachining tool (microSTRUCT™ Vario, 3D-Micromac AG, Chemnitz, Germany) for cutting through the substrates from the backside. The Ag-capped Si NP SERS substrates were stored in ambient conditions.

2.2. Scanning electron microscopy (SEM) analysis

Scanning electron microscopy (SEM) inspection was conducted using a Zeiss Supra VP 40 SEM (Zeiss, Oberkochen, Germany). The samples were imaged using an in-lens secondary electron detector in high vacuum mode and an acceleration voltage of 3 kV. Images were acquired with 50 K and 100 K magnification.

2.3. X-ray reflectometry (XRR) analysis

XRR analysis was performed for determining the deposited HfO_2 thicknesses on flat Si reference samples coated with the SERS substrates that were subject to 3, 6, 10, 15, 20, 25 and 150 ALD cycles. XRR was conducted using a Rigaku SmartLab 3 kW X-Ray Diffractometer (XRD) (Rigaku Corporation, Tokyo, Japan) which incorporates a high-resolution θ/θ closed loop goniometer drive system. XRR measurements were acquired using a Cu-Kα radiation source. The X-ray source was operated at a voltage of 40 kV and a current of 30 mA. The incident optics contained a 5° Soller slit, and an incident slit of 0.030 mm. The receiving optics comprised a 5° Soller slit, and two receiving slits of 0.030 mm and 0.075 mm. XRR 2θ/ω scans were recorded within the angular range of 0° - 8° with a step size of 0.01° and a measurement time of 5 s for each point. The fitting procedure was performed using SmartLab Studio II software (Rigaku Corporation, Tokyo, Japan) and a preloaded model stack composed of a Si substrate with a native oxide, a thin HfO_2 layer and a monolayer of water on the surface.

2.4. Finite element method (FEM) simulations

3D finite element method (FEM) was used for modelling Ag-capped Si NP dimers with varying HfO_2 thicknesses. The Wave Optics Module of COMSOL Multiphysics version 5.6 was used to numerically solve the Maxwell equations. A dimer composed of two neighbouring Ag-capped Si NPs covered by different thicknesses of HfO_2 was modelled in the software. The explicit dimensions pertaining to the Si NP geometry and the Ag cap morphology was extracted from SEM images of the produced SERS substrates. The minimum gap distance between the Ag caps was kept constant at 2 nm. Dielectric functions of Ag and HfO_2 were determined from references [29,30]. Perfectly matched layers were applied on the horizontal top and bottom boundaries of the solution domain to prevent non-physical reflections, whereas a Floquet periodicity boundary condition was used on all other boundaries of the domain. A normal incident plane wave from the top of the dimer was used for excitation. Its electrical field was polarized along the length-axis of the dimer.

2.5. X-ray photoelectron spectroscopy (XPS) analysis

XPS analysis was performed on Ag-capped Si NP substrates coated with HfO_2 using 10 and 15 ALD cycles. It was carried out on a Kratos Axis SUPRA spectrometer (Kratos Analytical Limited, Manchester, UK) using a monochromatic Al K_α x-ray source (1486.6 eV) with a pre-set acceleration voltage of 15 kV and an ion beam current of 8 mA. The instrument work function was calibrated to give a binding energy (BE) of 83.96 eV for the Au $4f_{7/2}$ line for metallic gold and the spectrometer dispersion was adjusted to give a BE of 932.62 eV for the Cu $2p_{3/2}$ line of metallic copper. The Kratos charge neutralizer system was used on all specimens. Survey scan analyses were carried out using an analysis area of 300 × 700 μm^2 and a pass energy of 160 eV. High resolution analyses were carried out using an analysis area of 300 × 700 μm^2 and a pass energy of 20 eV. The obtained spectra have been charge-corrected to the main line of the carbon 1 s spectrum (adventitious carbon) set to 284.8 eV, and they were analysed using Avantage software version 6.6 (Thermo Fisher Scientific, Waltham, MA, USA).

2.6. Scanning transmission electron microscopy coupled with energy-dispersive x-ray spectroscopy (STEM-EDS) analysis

STEM imaging was performed on Ag-capped Si NP substrates coated with HfO_2 using 10 and 15 ALD cycles. Prior to imaging, Focused Ion Beam (FIB) lamella preparation using a Dual Beam Helios 650 (Thermo Fisher Scientific, Waltham, MA, USA) was performed. The analysis was carried out in a probe-corrected Titan (Thermo Fisher Scientific, formerly FEI, Waltham, MA, USA) operated at 300 kV and equipped with a high brightness extreme field emission gun (X-FEG) and a spherical aberration Cs-corrector (CEOS) for the condenser system to provide sub-angstrom probe size. High angle annular dark-field (HAADF) STEM images were obtained using a HAADF detector. In this mode, the intensity of the signal is proportional to the square of the atomic number, which effectively enhances the brightness of heavy elements/atoms. Finally, in order to analyse the chemical composition of the materials, EDS, using a built-in Ultim Max detector (Oxford Instruments, Abingdon, Oxfordshire, UK), was combined with the STEM imaging. Point or area spectra, as well as chemical profiles (line scans) and 2D elemental maps were obtained this way. Data were further analysed with Aztec software (Oxford Instruments, Abingdon, Oxfordshire, UK).

2.7. Experimental procedure of stability test

The SERS performance stability of Ag-capped Si NP substrates coated with thin layers of HfO_2 (0, 3, 6, 10, 15, 20, 25 and 150 ALD cycles) was tested over a period ranging from 0 to 12 weeks with two SERS reporter molecules: BPE, and 4-NBT. BPE and 4-NBT were of technical grade and purchased from Sigma-Aldrich (Merck KGaA, Darmstadt, Germany). BPE powder was solubilized in ethanol to prepare a stock solution of 10 mM, and successively diluted in EtOH to 100 μM. 4-NBT powder was also solubilized in EtOH to prepare a stock solution of 10 mM. It was then diluted in EtOH to 1 μM. EtOH was of analytical grade and purchased from Sigma-Aldrich (Merck KGaA, Darmstadt, Germany).

During the 12-week period, all samples were stored in a desiccator at a reduced pressure of approximately 250 mbar. The SERS substrates were exposed to the two analytes using two different methods: (i) 2 μL analyte droplet casting using 100 μM BPE in EtOH and (ii) analyte incubation of 2 h in 150 μl of 1 μM 4-NBT. Five 3 × 3 mm^2 SERS chips were tested on a weekly basis with BPE, and on a biweekly basis with 4-NBT.

The SERS measurements were performed using a DXRxi Raman Imaging Microscope (Thermo Fisher Scientific, Waltham, MA, USA). SERS maps of the entire chip containing ~1000 spectra were acquired using a 780 nm excitation wavelength laser, 10X objective, laser power of 5 mW, exposure time of 0.05 s, 100 μm step size and 2 accumulations. The data analysis was performed using a custom-made Matlab SERS toolbox software package (2018b, MathWorks, MA, USA). Each spectrum in the maps was background corrected using a linear model in the 1570–1680 cm^{-1} spectral range for BPE, and in the 1520–1610 cm^{-1} spectral range for 4-NBT. The mean value of the characteristic BPE Raman mode vibration intensity at 1641 cm^{-1} (*C═C* stretch vibration [31]), and of the characteristic 4-NBT Raman mode vibration at 1570 cm^{-1} (CC stretch [32]) were calculated. The average of the peak intensity value was

extracted from 5 maps and obtained from the top 80 % of the data for each SERS map.

2.8. Experimental procedure 2,4-Dinitrophenol

To better evaluate the stability of Ag-capped Si NP SERS substrates coated with thin HfO_2 layers, the SERS performance of uncoated Ag-capped Si NP substrates was compared to the performance of Ag-capped Si NP substrates coated with 1.5 nm of HfO_2 (15 ALD cycles). To perform the evaluation, SERS substrates were exposed to a nitro-aromatic explosive DNP at two different time points: (i) right after SERS substrate fabrication, and (ii) five months after fabrication. In the period between measurements, all samples were stored in a desiccator at a reduced pressure of approximately 250 mbar. DNP was purchased from Sigma-Aldrich (≥98 % purity, moistened with water) and solubilized in methanol (MeOH) (analytical grade, VWR Chemicals BDH, VWR International, Radnor, Pennsylvania, USA) to prepare a 100 μM stock solution. The stock solution was diluted in Milli-Q water to prepare standards of 20 μM, 10 μM, 5 μM, 1 μM. A volume of 2 μl of DNP solutions was drop-casted on three SERS substrates per concentration and left to dry, while 2 μl of MeOH mixed with Milli-Q water (1:1 ratio) was drop-casted on three SERS substrates used as control samples.

The SERS measurements were performed using the previously mentioned DXRxi Raman Imaging Microscope. In this case, SERS maps of 2500 × 2500 μm^2 containing ~750 spectra were acquired using a 780 nm excitation wavelength laser, 10X objective, laser power of 10 mW, exposure time of 0.025 s, 100 μm step size and 3 accumulations. The data analysis was performed using a data analysis software developed using a combination of Delphi RAD Studio (Embarcadero Technologies, Austin, TX, USA) and Python (Python Software Foundation, Wilmington, Delaware, USA). The collected spectra were cropped between 500 cm^{-1} and 2000 cm^{-1}, filtered and background corrected with a rolling-circle filter (wheel radius=350, elliptic coefficient=2). The characteristic DNP spectral feature at 830 cm^{-1} ($2NO_2$ scissoring + in-plane ring bending [33]) was considered during analysis. An average of the intensity values of the peak was extracted from 3 maps, in which an intensity threshold was applied in order to consider only the droplet region on the SERS substrate surface. The data were plotted and fitted using a linear function with Origin (2023, OriginLab Corporation, MA, USA).

The theoretical limits of detection (LoD) for the different types of substrates were calculated on 4 points as $3\sigma/s$, in which σ is the standard deviation (SD) of the intercept of the linear range, and s is the slope of the calibration curve. The limits of quantification (LoQ) were calculated as $10\sigma/s$. A statistical test (t-test) was implemented on the slopes of the two calibration curves of the HfO_2-coated substrates to check the similarity between the two. The two slopes and the standard deviation of the slopes were considered.

3. Results and discussion

3.1. Characterization results

The characterization process started with the acquisition of SEM images (Fig. 1) to calculate the density and the height of Si NPs and to assess the morphology of the Ag caps. Fig. 1a and Fig. 1b show SEM images of the final SERS substrates after the HfO_2 deposition using 10 ALD cycles. The NP density was approximately 21 NP/μm^2. From an average of 9 measurements on different pillars after metal deposition, the NP height with the metal cap was approximately 916.9 ± 29 nm and

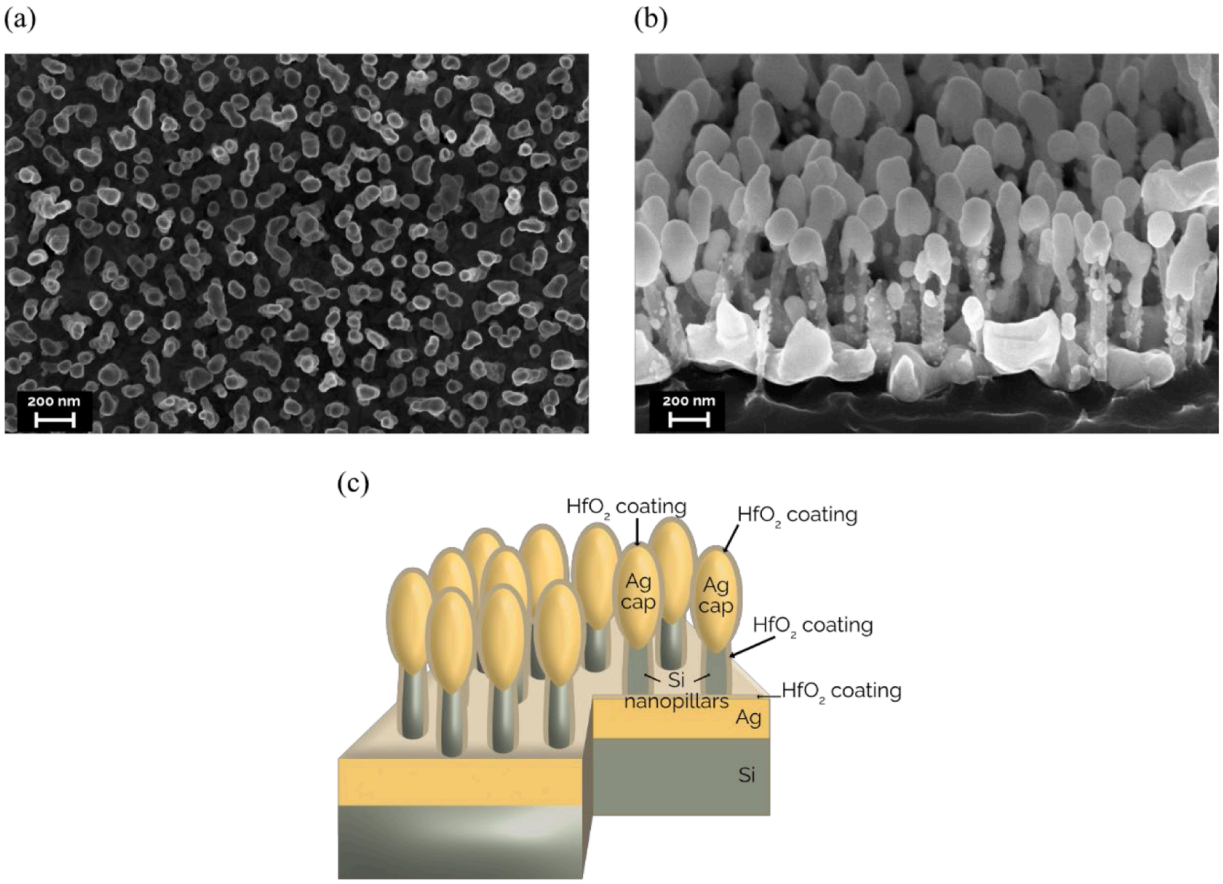

Fig. 1. SEM images of Ag-capped Si NPs coated with 1.2 nm HfO_2. (a) Top-down view of Ag-capped Si NPs coated with 1.2 nm HfO_2. (b) Tilted view (30°) of Ag-capped Si NPs coated with 1.2 nm HfO_2. (c) Schematic representation of Ag-capped Si NPs featuring a thin HfO_2 protective coating.

the metal cap measured approximately 236.2 ± 24 nm. Fig. 1b shows that the Si NPs were coated with metal caps having a smooth surface morphology, which conformed well to the shape of the pillar covering the top of them. However, some metal deposited or redeposited on the sides of the NPs.

From the SEM images, it was not possible to extract any meaningful data pertaining to the thin HfO_2 coating. A schematic representation of how the layer should ideally cover the Ag-capped Si NPs is shown in Fig. 1c.

To evaluate the HfO_2 thickness obtained after deposition using a varying number of ALD cycles, XRR analysis was performed. XRR is a non-destructive analysis technique used to determine thin layer structural properties, such as thickness, density and roughness. Flat Si references covered with native SiO2 and subsequently coated with HfO2 using different numbers of ALD cycles were employed for the analysis. X-ray reflectivity measurements rely on the interference of X-rays reflected from the interfaces of thin films. At grazing incidence angles, total external reflection occurs below a specific critical angle, which depends on the electron density of the material. As the angle increases beyond this critical angle, X-rays penetrate the film and are reflected from the interfaces between different layers. In this case, interference between the X-rays reflected from the air/HfO2 and HfO2/SiO2 interfaces produces an oscillation pattern known as Kiessig fringes, which is visible in Figure S1a. These fringes provide information on the thickness, density, and roughness of the thin films. The oscillation patterns were fitted using SmartLab Studio II software using a model comprising a Si substrate with SiO_2 and the deposited HfO_2 layer with a monolayer of H_2O (Figure S1b). The thickness, density and roughness obtained from analysing substrates coated with HfO_2 using different numbers of ALD cycles are shown in Table 1.

The XRR data pertaining to the HfO_2 thicknesses associated with a varying number of ALD cycles was utilized to gain a more profound understanding of how the thin protective coating could impact the SERS performance through a decrease in EM field enhancement at the surface of the plasmonic Ag caps and more specifically in hot spots between neighbouring Ag caps. FEM was employed for the simulation of the maximum EM field enhancement associated with the plasmonic hotspot formed by two neighbouring Ag-capped Si NPs covered by a thin film of HfO_2 with thickness (T_{HfO2}) varying from 0–6 nm.

Fig. 2 shows that there are four localized surface plasmon resonance (LSPR) modes for a dimer of Ag-capped Si NPs covered by a thin film of HfO_2, noted by M1, M2, M3, and M4. With increased HfO_2 thickness (T_{HfO2}), all these modes experience red shifts, accompanied by decreased intensity. For further understanding, Figure S2 plots the corresponding electrical field distributions. An LSPR mode with more electromagnetic energy in the HfO_2 film experiences a stronger red shift when T_{HfO2} increases, due to significant changes in the dielectric environment. In addition, an increased T_{HfO2} weakens the interaction between the Ag cores in the dimer, leading to a decrease in the electric field enhancement.

Considering the simulation results, a HfO_2 layer thickness of 1–1.5 nm was chosen for further characterization to avoid a potentially too low electrical field enhancement. The samples coated using 10 and 15 ALD cycles were analysed using XPS to assess the presence of HfO_2 and to determine its chemical state. The analysis confirmed the presence of HfO_2 on the surface of the substrate after the deposition, as shown in Fig. 3 for the substrate coated using 15 ALD cycles. The chemical state of Hf in the oxide is characterized by the Hf 4*f* peaks, which represent the core level photoelectron signals emitted from the 4*f* orbitals of Hf atoms (Fig. 3). As evident from Fig. 3, the Hf 4*f* region has a well separated spin-orbit component.

The atomic percentage of Hf 4*f* is shown in Table 2 and it was approximately 5.64 %, which might be overestimated since only the surface of the sample was analysed. To better quantify the presence of HfO_2, STEM-EDS was employed. The same XPS analysis was carried out on Ag-capped Si NP SERS substrates coated using 10 ALD cycles (Figure S3), which gave an atomic percentage of Hf 4*f* equal to 3.78 %, confirming the presence of an even thinner layer on the surface (Table S1).

To investigate whether a conformal HfO_2 coating exhibiting a uniform thickness was obtained, STEM-EDS analysis was performed on HfO_2-coated Ag-capped Si NP SERS substrates subject to 10 and 15 cycles of ALD. After fabricating the lamella, two different sites per substrate were analysed. The analysis at Site 1 of a HfO_2-coated Ag-capped Si NP SERS (15 ALD cycles) substrate can be seen in Fig. 4, while the analysis on Site 2 is shown in Figure S4. The STEM-EDS analysis on HfO_2-coated Ag-capped Si NP SERS substrates using 10 ALD cycles is shown in Figure S5 and S6.

Fig. 4b shows the EDS layered image associated with Site 1. From the electron image (Fig. 4c) and the EDS images showing the distribution of Ag (Fig. 4d) and Hf (Fig. 4e) it was possible to estimate the thickness of the ultra-thin layer of HfO_2 deposited on the actual Ag caps. The measurement confirmed the results from the XRR measurements on flat samples, giving a value of ~1.5 nm. Similarly, the measurements from 10 ALD cycles HfO_2-coated Ag-capped Si NP SERS substrates gave a value of 1.2 nm (Figure S5c), in accordance with the XRR results.

At Site 1, three areas were selected to collect different EDS spectra at the metal cap to better examine the presence of Hf. Table 3 shows the EDS weight percentage of the element in the sample as the average of the three areas in which the EDS spectra were collected. As it is possible to observe, Hf presence was confirmed in the substrate with a weight percentage of 4.57 %, showing a higher value in the HfO_2-coated Ag substrate using 15 ALD cycles than in the one coated using 10 ALD cycles (3.19 %, Table S2) confirming a slightly thicker coating.

The presence of Pt derives from the lamella fabrication process, in which Pt was deposited using Focused Electron Beam Induced Deposition (FEBID) and Focused Ion Beam Induced Deposition (FIBID). Cu is also a parasitic signal since it is coming from the Titan equipment, in particular from the grating where the samples are mounted. Moreover, the low percentages of Fe and Co correspond to the polar part of the objective lens. When measuring with an angle $\alpha = 0$ this signal becomes visible, while it usually disappears when $\alpha = 20^{\circ}$ Therefore, we can discard these Fe and Co signals as secondary signals coming from the equipment. Instead, the presence of S can be caused by etching by-products, which might be more uniformly distributed in deeper regions of the NPs and detectable with EDS.

Table 1
HfO2 layer thickness, density and roughness as a function of the number of ALD cycles.

XRR analysis			
HfO_2 ALD cycles	Thickness, nm	Density, g/cm^3	Roughness, nm
3	0.86	6.89	0.49
6	1.01	7.53	0.24
10	1.21	7.84	0.27
15	1.55	8.69	0.25
20	1.76	7.07	0.20
25	2.15	7.78	0.37
150 - Reference	13.11	5.63	0.35

3.2. Stability test

The characterization of the HfO_2-coated SERS substrates also involved an evaluation of their SERS performance and their SERS signal stability over time. Since HfO_2 is a wide band-gap semiconductor, the applied laser wavelength of 785 nm did not induce an electronic transition in HfO_2.In the stability study, all samples covered by 0–13 nm thick coatings were tested over a period ranging from 0 to 12 weeks by drop casting 2 μl of 100 μM BPE solution on new pieces of substrate weekly, and by incubating them for 2 h in 1 μM 4-NBT solution every two weeks. This second test, in which the substrates were incubated in

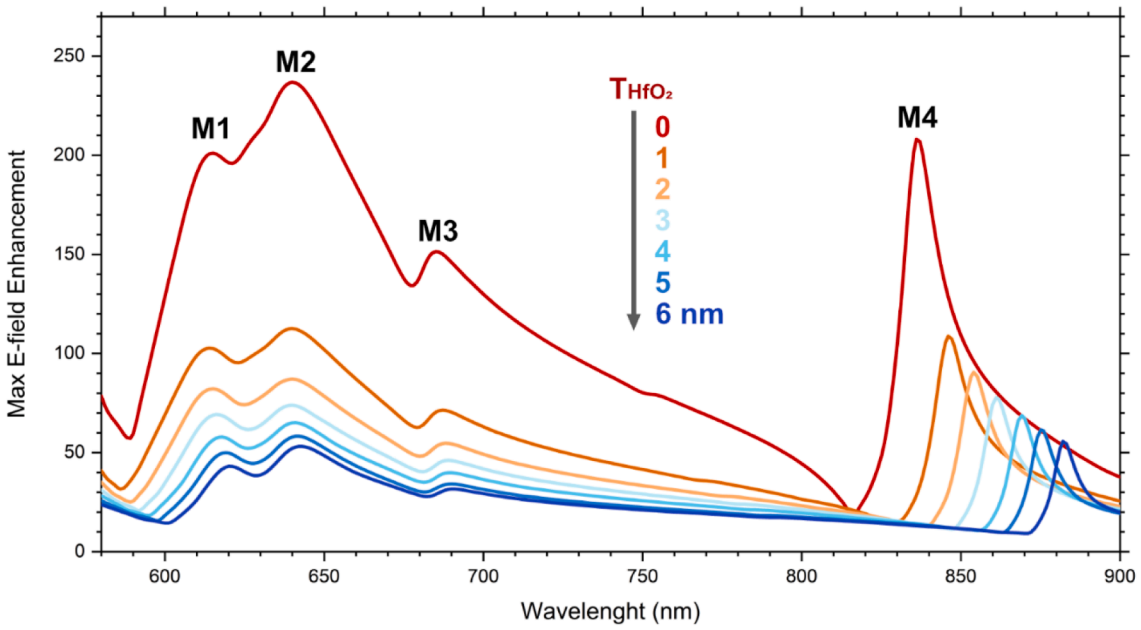

Fig. 2. Simulated maximum electrical field enhancement associated with the plasmonic hotspot formed by two neighbouring Ag-capped Si NPs covered by a thin film of HfO_2 with thickness T_{HfO2} varying from 0 to 6 nm.

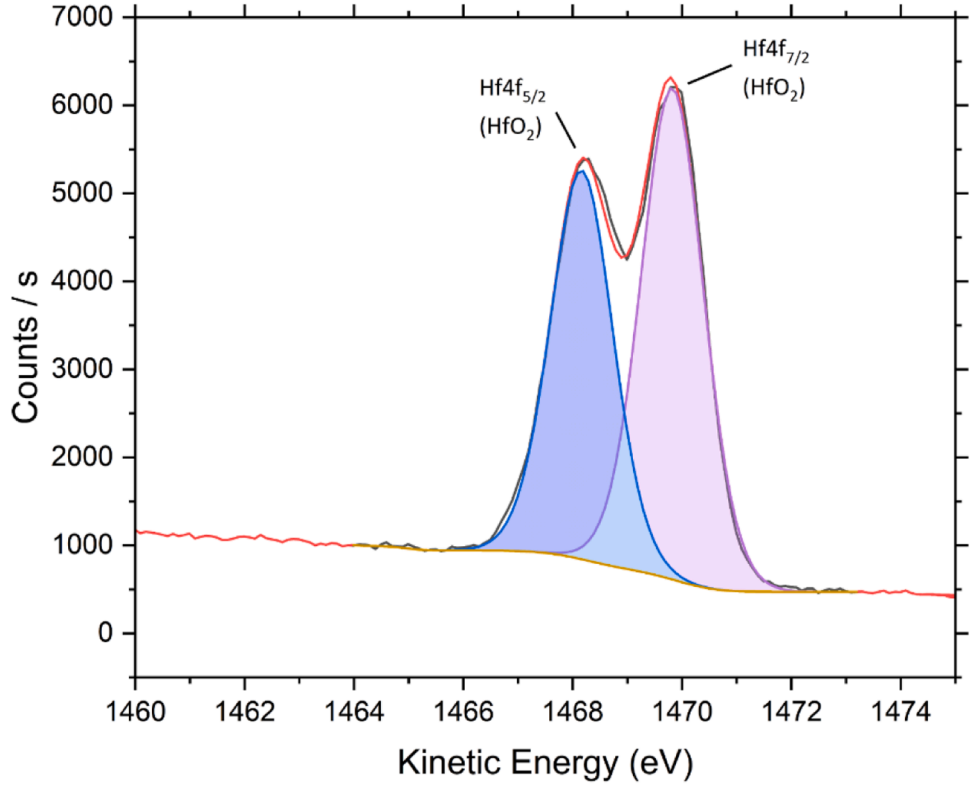

Fig. 3. XPS analysis of Hf 4f peak in HfO_2-coated Ag-capped Si NP SERS substrate using 15 ALD cycles.

low concentration of 4-NBT, was performed to evaluate the homogeneity of the HfO_2 coating.

Figure S7a and Figure S7b show that 100 μM BPE was detected using substrates coated using up to 20 ALD cycles. The BPE SERS signal intensity at 1641 cm^{-1} ($C{=}C$ stretch vibration [31]) gradually decreased as a function of the increased HfO_2 layer thickness, as expected. Since the electromagnetic field strength decreases exponentially with distance from the Ag metal surface, the dielectric layer introduced between the analyte molecules and the Ag-metal surface reduces and modulates the electromagnetic field enhancement and therefore the SERS intensity. The uncoated Ag-capped Si NP SERS substrates (0 ALD cycles) displayed very unstable performance over the period of 12 weeks confirming poor physicochemical stability of Ag. HfO_2-coated substrates showed a relatively stable performance over time. The sample coated using 15 ALD cycles displayed a relatively stable SERS intensity at approximately 500 $cts*(mW*s)^{-1}$ over the entire 3-month measurement period.

Table 2
XPS Atomic percentage of elemental composition in HfO_2-coated SERS substrates using 15 ALD cycles.

XPS	Atomic percentage (%)
Element	**15 ALD cycles**
Hf *4f*	5.64
Si *2s*	1.16
C *1s*	33.25
Ag *3d*	18.64
O *1s*	37.51
F *1s*	3.80

In the second test, shown in Figure S7c-d, the SERS performance of the same HfO_2-coated Ag-capped Si NP substrates was evaluated using the characteristic 4-NBT Raman mode vibration at 1570 cm^{-1} (CC stretch [32]). The uncoated Ag-capped Si NP SERS substrates (0 ALD cycles) displayed the same instability as in the BPE experiment, while the 15 ALD cycles HfO_2-coated Ag-capped Si NP SERS substrates showed a better stability but a significant decrease in sensitivity. However, some background noise and especially the background peak at 960 cm^{-1} associated with sulphur-containing organic compounds [34,35] were successfully removed using HfO_2-coated Ag NP SERS substrates (15 ALD cycles).

Therefore, both tests using two different analytes (BPE, 4-NBT) and two different molecule deposition approaches (drop casting, incubation) showed that the uncoated Ag NP substrate performance varied significantly as a function of sample storage time. The Ag NP SERS substrate coated using 15 ALD cycles which correspond to approximately 1.5 nm thick HfO_2 layer showed the most stable SERS performance.

3.3. 2,4-Dinitrophenol test

The SERS detection capabilities of HfO_2-coated Ag-capped Si NP substrates were evaluated using the explosive DNP and in particular its characteristic spectral feature at 830 cm^{-1} ($2NO_2$ scissoring and in-plane ring bending [33]). The analysis sought to compare the SERS performance of uncoated Ag-capped Si NP substrates with the SERS performance of HfO_2-coated Ag-capped Si NP SERS substrates (15 ALD cycles),

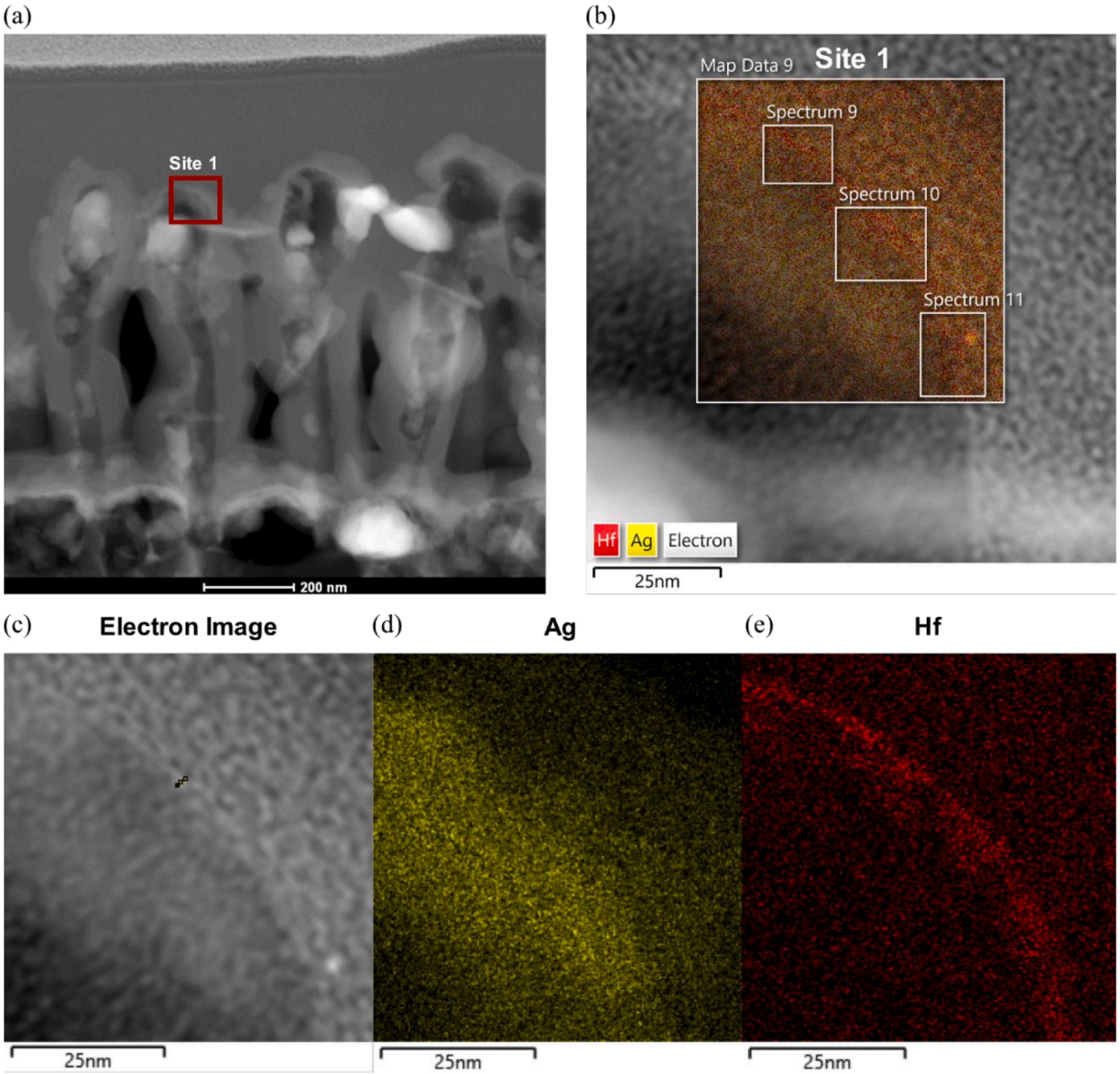

Fig. 4. (a) TEM image of HfO_2-coated Ag-capped Si NP SERS substrate (15 ALD cycles) lamella – The sites analysed (Site 1 is highlighted). (b) Site 1 EDS layered image with EDS spectra location highlighted. (c) Site 1 electron image with HfO_2 calculated thickness. (d) Site 1 EDS image showing Ag distribution. (e) Site 1 EDS image showing Hf distribution.

Table 3
EDS weight percentage of elemental composition in HfO_2-coated SERS substrates using 15 ALD cycles.

EDS	Weight percentage (%)
Element	**15 ALD cycles – Site 1**
C	8.68 ± 0.46
O	1.74 ± 0.15
S	3.31 ± 0.17
Fe	0.97 ± 0.10
Co	0.99 ± 0.11
Cu	5.86 ± 0.25
Ag	22.37 ± 0.51
Hf	4.57 ± 0.54
Pt	51.50 ± 0.70

right after substrate fabrication, and five months thereafter.

Fig. 5a shows the averaged SERS spectra of maps recorded after drop casting 2 µl of 20 µM, 10 µM, 5 µM and 1 µM DNP solution on HfO_2-coated Ag-capped Si NP SERS substrates (15 ALD cycles). The intensity of DNP characteristic peak (enlarged in Fig. 5b) is linearly increasing with the concentration. In Fig. 5c, the averaged SERS spectra of 10 µM DNP solution recorded on an uncoated Ag-capped Si NP substrate right after fabrication (black spectra and y-axis) is compared to the spectra of 10 µM DNP recorded on a HfO_2-coated Ag-capped Si NP SERS substrate (15 ALD cycles) (red spectra and y-axis). The spectra of uncoated Ag-capped Si NP substrates showed a higher intensity as expected from the previous stability test. However, part of the background noise (i.e. the peak at 1150 cm^{-1} interfering with the analyte peak at around 1320 cm^{-1}) and especially the background peak at 960 cm^{-1} were not present when using HfO_2-coated Ag-capped Si NP substrates (15 ALD cycles).

To determine the effects of the HfO_2 coating in terms of preventing surface contamination, DNP 830 cm^{-1} characteristic band signal intensity vs. concentration curves on uncoated Ag-capped Si NP substrates right after fabrication and five months after fabrication were constructed and compared to the ones of HfO_2-coated Ag-capped Si NP substrates. A linear correlation between concentration and intensity was obtained between 1 µM and 20 µM for uncoated and coated substrates (Fig. 6). Table S3 summarises the figures of merit for Ag-capped Si NP substrates and HfO_2-coated Ag-capped Si NP substrates (15 ALD cycles) for both time points (T0 – T5 months).

As shown in Fig. 6a, the uncoated Ag-capped Si NP substrates displayed the highest sensitivity right after fabrication, with a theoretical LoD and LoQ of 0.31 µM and 1.04 µM, respectively. However, they also showed the largest substrate-to-substrate SERS signal variance with an RSD of 45 %. A lower SERS sensitivity was observed using HfO_2-coated Ag-capped Si NP substrates since a ~1.5 nm gap between DNP molecules and Ag-metal was introduced. The theoretical LoD and LoQ were 2.95 µM and 9.83 µM, respectively. However, even in this case, DNP was still detectable down to 1 µM, when considering the concentration that gives a response of three times the signal intensity of the blank sample. Moreover, the HfO_2-coated substrate exhibited a lower substrate-to-substrate SERS signal variance with an RSD of 19 %.

When the measurements were repeated five months after substrate fabrication (Fig. 6b), the performance of uncoated Ag-capped Si NP substrates drastically dropped, confirming the poor stability of Ag. The theoretical LoD and LoQ were calculated, giving values of 3.09 µM and 10.30 µM, respectively, comparable to the ones of HfO2-coated Ag-capped Si NP substrates (15 ALD cycles) which were 4.24 µM and 14.12 µM. Therefore, after 5 months storage, the sensitivity of uncoated Ag became comparable to the one of HfO_2-coated Ag. Moreover, the HfO_2-coated Ag-capped Si NP substrates (15 ALD cycles) showed a good stability, giving almost the same results after 5 months, as shown in Fig. 6c. These findings are essential in laboratory settings where it is important to compare results from different time points and ensure that substrates remain stable and provide reliable results over time. To quantify the similarity of the SERS performance of HfO_2-coated Ag-capped Si NP substrates (15 ALD cycles) at T0 and T5, a statistical test (*t*-test) was implemented on the slopes of the two calibration curves of the HfO_2-coated Ag-capped Si NP substrates at the two time points, also taking into account the standard deviation of the slopes. It was found that the reported p-value was higher than 0.05, which indicated that the slopes or sensitivity of the two calibrations did not have significant differences. The results showed a fair degree of stability, confirming that the coating of Ag nanostructures represents a strategy to improve the chemical stability of Ag. Moreover, the possibility to tune the coating can lead to an even higher sensitivity.

4. Conclusions

In the present study, we evaluated the production and characterization of Ag-capped Si NP SERS substrates featuring thin protective HfO_2 coatings with potential applications as temporally stable SERS substrates. For the HfO_2 deposition, ALD was employed to prepare

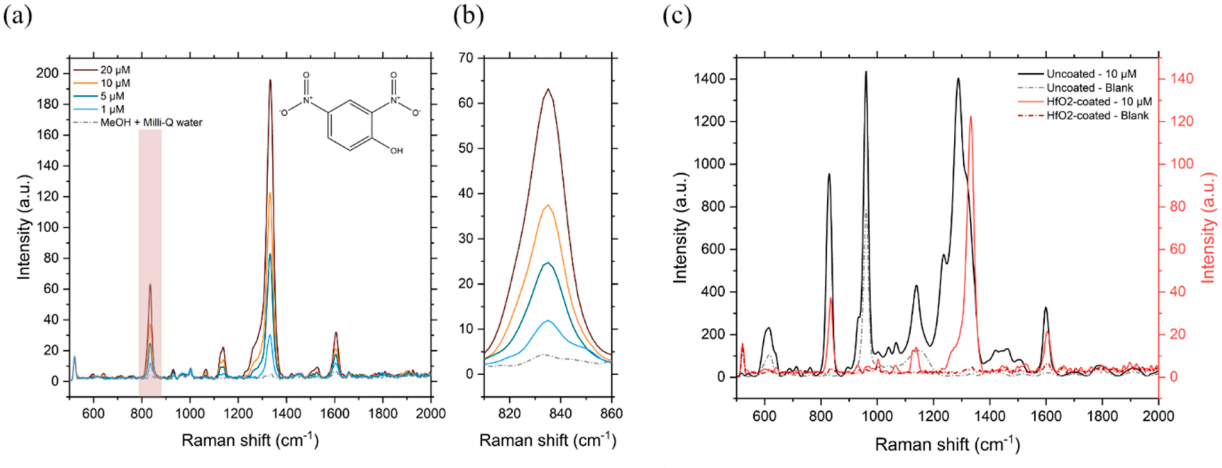

Fig. 5. (a) Averaged SERS spectra of DNP in MeOH diluted in Milli-Q water, and of MeOH diluted in Milli-Q water (control sample) recorded from HfO_2-coated Ag-capped Si NP SERS substrates coated using 15 ALD cycles. DNP chemical structure is displayed in the inset. (b) Concentration-dependent intensity of the peak at 830 cm^{-1} for DNP. (c) Averaged SERS spectra after drop casting 2 µl of 10 µM DNP solution on uncoated Ag-capped Si NP SERS substrates (black line), 2 µl of 10 µM DNP solution on 15 ALD cycles HfO_2-coated Ag-capped Si NP SERS substrates (red line), 2 µl of MeOH+Milli-Q water on uncoated Ag-capped Si NP SERS substrates (grey dashed line), and 2 µl of MeOH+Milli-Q water on 15 ALD cycles HfO_2-coated Ag-capped Si NP SERS substrates (red dashed line). Spectra from 15 ALD cycles HfO_2-coated Ag-capped Si NP SERS substrates are shown on the secondary (red) y-axis.

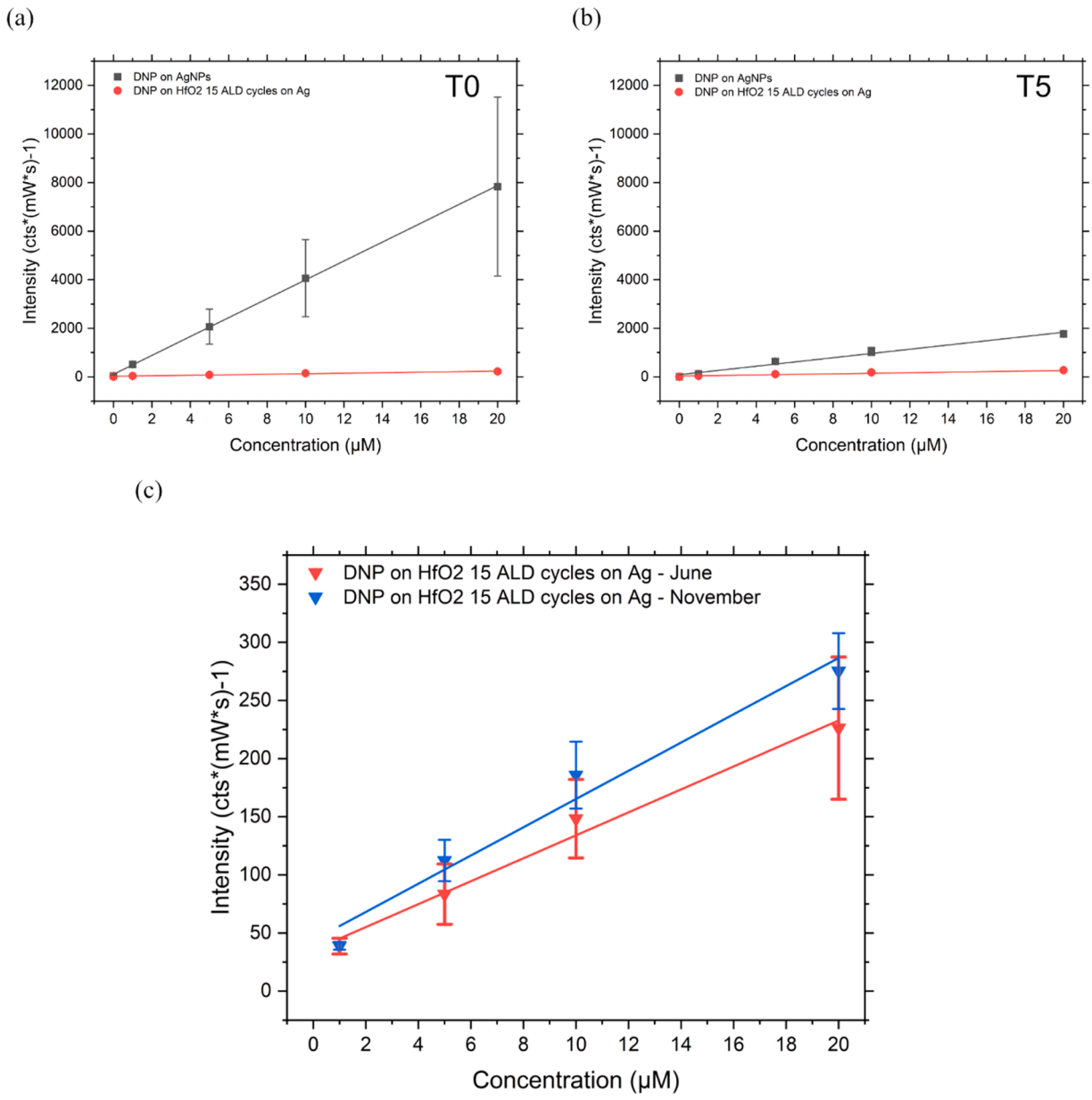

Fig. 6. (a) Comparison of the peak intensity vs. concentration curve of the 830 cm^{-1} peak SERS signal of DNP recorded from uncoated Ag NP SERS substrates right after fabrication and from 15 ALD cycles HfO_2-coated Ag NP SERS substrates ($n = 3$). (b) Comparison of the peak intensity vs. concentration curve of the 830 cm^{-1} peak SERS signal of DNP recorded from uncoated Ag NP SERS substrates 5 months after fabrication and from 15 ALD cycles HfO_2-coated Ag NP SERS substrates ($n = 3$). (c) Comparison of the peak intensity vs. concentration curve of the 830 cm^{-1} peak SERS signal of DNP recorded over a 5-month interval from 15 ALD cycles HfO_2-coated Ag NP SERS substrates ($n = 3$).

samples with different thicknesses ranging from 0–13 nm. The substrates and in particular the substrate surfaces were characterized using an ensemble of different techniques including SEM, XRR, XPS, STEM-EDS, and 3D FEM modelling. From the characterization results, the substrates coated using 10 and 15 ALD cycles presented a thin and conformal HfO_2 layer having approximate thicknesses of 1.2 nm and 1.5 nm, respectively.

The SERS performance of all coated substrates was tested in terms of (i) long-term signal stability, (i) background noise reduction, and (iii) overall signal intensity using two reporter molecules BPE, and 4-NBT over a period of 12 weeks. Both tests using the two different analytes showed that the uncoated Ag-capped Si NP substrate performance varied significantly as a function of sample storage time, while the substrates coated with ~1.5 nm HfO_2 were superior in terms of signal stability and background noise reduction.

In order to test the substrate stability in a real-world scenario, the detection of different concentrations of DNP was investigated. A performance comparison between substrates coated with 1.5 nm HfO_2 and uncoated substrates was performed at two time points: (i) right after fabrication, and (ii) five months after fabrication. At first, HfO_2-coated substrates using 15 ALD cycles presented a reduced sensitivity, with a theoretical LoD and LoQ of 2.95 μM and 9.83 μM, respectively. These values were higher than the theoretical LoD and LoQ of uncoated substrates (0.31 μM and 1.04 μM, respectively). However, the uncoated substrates also showed the largest chip-to-chip SERS signal variance with an RSD of 45 %. The lower SERS sensitivity observed using HfO_2-coated substrates was due to the ~1.5 nm gap between DNP molecules and Ag-metal. The same test performed 5 months after fabrication showed a large decay of the SERS performance of uncoated Ag-capped Si NPs. The theoretical LoD and LoQ calculated again (3.09 μM and 10.30

μM, respectively) were comparable to the ones of HfO2-coated Ag NPs (4.24 μM and 14.12 μM). Therefore, in 5 months the sensitivity of uncoated Ag is comparable with the one of HfO_2-coated structures with the crucial difference that HfO_2-coated substrates showed stable SERS performance.

In conclusion, protective layers can represent an effective strategy to improve the structural and chemical stability of Ag. However, more optimization is needed to tune the coating to improve the sensitivity and to reach an even better stability.

CRediT authorship contribution statement

Giulia Zappalà: Writing – review & editing, Writing – original draft, Visualization, Validation, Project administration, Methodology, Investigation, Formal analysis, Data curation, Conceptualization. **Lasse Højlund Eklund Thamdrup:** Writing – review & editing, Validation, Supervision, Methodology. **AmirAli Abbaspourmani:** Writing – review & editing, Methodology, Investigation, Formal analysis. **Elodie Dumont:** Writing – review & editing, Validation, Supervision, Project administration, Methodology. **Kaiyu Wu:** Writing – review & editing, Validation, Methodology, Formal analysis. **Evgeniy Shkondin:** Writing – review & editing, Validation, Methodology, Investigation, Formal analysis. **Reyes Mallada:** Writing – review & editing, Validation, Supervision, Resources, Methodology, Investigation. **Maria Pilar Pina:** Writing – review & editing, Validation, Supervision, Resources, Methodology, Investigation. **Tomas Rindzevicius:** Validation, Resources, Project administration, Funding acquisition, Conceptualization. **Anja Boisen:** Writing – review & editing, Supervision, Resources, Project administration, Funding acquisition.

Declaration of competing interest

The authors declare the following financial interests/personal relationships which may be considered as potential competing interests:

Giulia Zappala' reports financial support was provided by European Union's Horizon 2020 Research and Innovation Programme. Anja Boisen has patent Surface enhanced Raman scattering substrates consumables for Raman spectroscopy licensed to Technical University of Denmark. If there are other authors, they declare that they have no known competing financial interests or personal relationships that could have appeared to influence the work reported in this paper.

Acknowledgements

The authors acknowledge financial support from the European Union's Horizon 2020 Research and Innovation Programme (Grant Agreement No 883390 H2020-SU-SECU-2019 SERSing Project).

The authors also acknowledge the use of instrumentation as well as the technical advice provided by the National Facility ELECMI ICTS node " Laboratorio de Microscopías Avanzadas" at the University of Zaragoza. Specific acknowledgements go to Rodrigo Fernández-Pacheco (Laboratorio de Microscopías Avanzadas, Universidad de Zaragoza) for STEM-EDS analysis, Laura Casado (Laboratorio de Microscopías Avanzadas, Universidad de Zaragoza) for STEM sample preparation, and Guillermo Antorrena (Laboratorio de Microscopías Avanzadas, Universidad de Zaragoza) for XPS analysis.

Supplementary materials

Supplementary material associated with this article can be found, in the online version, at doi:10.1016/j.surfin.2025.106415.

Data availability

Data will be made available on request.

References

[1] R. Pilot, et al., A review on surface-enhanced Raman scattering, Biosensors (Basel) 9 (2019).
[2] A. Orlando, et al., A comprehensive review on raman spectroscopy applications, Chemosensors 2021 9 (2021) 262. *Vol. 9, Page 262*.
[3] E.C. Le Ru, P.G. Etchegoin, Principles of surface-enhanced raman spectroscopy, Principles Surface-Enhanced Raman Spectroscopy (2009), https://doi.org/10.1016/B978-0-444-52779-0.X0001-3.
[4] E. Hao, G.C. Schatz, Electromagnetic fields around silver nanoparticles and dimers, J. Chem. Phys. 120 (2004) 357–366.
[5] S.Y. Ding, E.M. You, Z.Q. Tian, M. Moskovits, Electromagnetic theories of surface-enhanced raman spectroscopy, Chem. Soc. Rev. 46 (2017) 4042–4076.
[6] A.I. Pérez-Jiménez, D. Lyu, Z. Lu, G. Liu, B. Ren, Surface-enhanced Raman spectroscopy: benefits, trade-offs and future developments, Chem. Sci. 11 (2020) 4563–4577.
[7] B. Sharma, R.R. Frontiera, A.I. Henry, E. Ringe, R.P. Van Duyne, SERS: materials, applications, and the future, Mater. Today 15 (2012) 16–25.
[8] P.R. West, et al., Searching for better plasmonic materials, Laser Photon Rev 4 (2010) 795–808.
[9] K.M. Mayer, J.H. Hafner, Localized surface plasmon resonance sensors, Chem. Rev. 111 (2011) 3828–3857.
[10] A.S. Preston, R.A. Hughes, N.L. Dominique, J.P. Camden, S. Neretina, Stabilization of plasmonic silver nanostructures with ultrathin oxide coatings formed using atomic layer deposition, J. Phys. Chem. C 125 (2021) 17212–17220.
[11] A. Matikainen, et al., Atmospheric oxidation and carbon contamination of silver and its effect on surface-enhanced Raman spectroscopy (SERS), Sci. Rep. 6 (2016) 1–6. *2016 6:1*.
[12] H. Kang, et al., Stabilization of silver and gold nanoparticles: preservation and improvement of plasmonic functionalities, Chem. Rev. 119 (2019) 664–699.
[13] X. Wang, et al., Simultaneously improved SERS sensitivity and thermal stability on Ag dendrites via surface protection by atomic layer deposition, Appl. Surf. Sci. 611 (2023) 155626.
[14] W. Bian, et al., High reliable and robust ultrathin-layer gold coating porous silver substrate via galvanic-free deposition for solid phase microextraction coupled with surface enhanced Raman spectroscopy, Anal. Chim. Acta 994 (2017) 56–64.
[15] C. Gao, et al., Highly stable silver nanoplates for surface plasmon resonance biosensing, Angewandte Chemie - Int. Edition 51 (2012) 5629–5633.
[16] J. Prakash, H.C. Swart, G. Zhang, S. Sun, Emerging applications of atomic layer deposition for the rational design of novel nanostructures for surface-enhanced Raman scattering, J. Mater. Chem. C 7 (2019) 1447–1471, https://doi.org/10.1039/C8TC06299D. Preprint at.
[17] X. Kong, et al., Synthesis and application of surface enhanced raman scattering (SERS) tags of Ag@SiO2 core/shell nanoparticles in protein detection, J. Mater. Chem. 22 (2012) 7767–7774.
[18] L. Ma, Y. Huang, M. Hou, Z. Xie, Z. Zhang, Ag nanorods coated with ultrathin TiO2 shells as stable and recyclable SERS substrates, Sci. Rep. 5 (2015) 1–8. *2015 5:1*.
[19] L. Ma, Y. Huang, M. Hou, Z. Xie, Z. Zhang, Silver nanorods wrapped with ultrathin Al2O3 layers exhibiting excellent SERS sensitivity and outstanding SERS stability, Sci. Rep. 5 (2015) 1–9. *2015 5:1*.
[20] S. Wang, et al., HfO2-wrapped slanted Ag nanorods array as a reusable and sensitive SERS substrate for trace analysis of uranyl compounds, Sens Actuat. B Chem. 265 (2018) 539–546.
[21] L. Ma, J. Li, S. Zou, Z. Zhang, Ag nanorods-oxide hybrid array substrates: synthesis, characterization, and applications in surface-enhanced raman scattering, Sensors 17 (2017) 1895. *2017, Vol. 17, Page 1895*.
[22] Q. Tong, W. Wang, Y. Fan, L. Dong, Recent progressive preparations and applications of silver-based SERS substrates, TrAC Trends Anal. Chem. 106 (2018) 246–258.
[23] Y. Zheng, et al., Surface-enhanced raman scattering (SERS) substrate based on large-area well-defined gold nanoparticle arrays with high SERS uniformity and stability, Chempluschem 79 (2014) 1622–1630.
[24] W. Kim, et al., An excitation wavelength-optimized, stable SERS biosensing nanoplatform for analyzing adenoviral and AstraZeneca COVID-19 vaccination efficacy status using tear samples of vaccinated individuals, Biosens. Bioelectron. 204 (2022).
[25] X. Zhang, et al., Surface-enhanced Raman spectroscopy for environmental monitoring using gold clusters anchored on reduced graphene oxide, Sci. Total Environ. 856 (2023) 158879.
[26] S. Botti, L. Cantarini, A. Palucci, Surface-enhanced Raman spectroscopy for trace-level detection of explosives, J. Raman Spectrosc. 41 (2010) 866–869.
[27] S. Chatterjee, U. Deb, S. Datta, C. Walther, D.K. Gupta, Common explosives (TNT, RDX, HMX) and their fate in the environment: emphasizing bioremediation, Chemosphere 184 (2017) 438–451.
[28] M.S. Schmidt, et al., Large area fabrication of leaning silicon nanopillars for surface enhanced raman spectroscopy, Adv. Mater. 24 (2012) OP11–OP18.
[29] P.B. Johnson, R.W. Christy, Optical constants of the noble metals, Phys. Rev. B 6 (1972) 4370.
[30] M.F. Al-Kuhaili, Optical properties of hafnium oxide thin films and their application in energy-efficient windows, Opt Mater (Amst) 27 (2004) 383–387.
[31] Z. Zhuang, et al., Density functional theory calculation of vibrational spectroscopy of trans-1,2-bis(4-pyridyl)-ethylene, Vib. Spectrosc. 43 (2007) 306–312.
[32] Y. Zhang, Y. Hu, G. Li, R. Zhang, A composite prepared from gold nanoparticles and a metal organic framework (type MOF-74) for determination of 4-nitrothiophenol by surface-enhanced Raman spectroscopy, Microchim. Acta 186 (2019).

[33] V. Chiș, Molecular and vibrational structure of 2,4-dinitrophenol: FT-IR, FT-raman and quantum chemical calculations, Chem. Phys. 300 (2004) 1–11.
[34] Y. Matsumoto, et al., Raman spectroscopic study of aqueous alkali sulfate solutions at high temperature and pressure to yield precipitation, J. Supercrit. Fluids 49 (2009) 303–309.
[35] K. Ben Mabrouk, T.H. Kauffmann, H. Aroui, M.D. Fontana, Raman study of cation effect on sulfate vibration modes in solid state and in aqueous solutions, J. Raman Spectrosc. 44 (2013) 1603–1608.